Theoretical analysis of tissue axial stretching model in elastography*

LUO Jianwen[1], DING Chuxiong[1], BAI Jing[1]** and HE Ping[2]

(1. Department of Biomedical Engineering, Tsinghua University, Beijing 100084, China; 2. Department of Biomedical, Industrial, and Human Factors Engineering, Wright State University, Dayton, Ohio 45435-0001, USA)

Received September 3, 2003; revised October 28, 2003

Abstract The performance of axial displacement estimation in ultrasound elastography can be degraded by tissue lateral displacements, mainly because of the move-in and move-out of tissue scatterers. In our previous work, a tissue axial stretching model was proposed to separate the decorrelation effect induced by lateral displacements from other decorrelation sources. In this paper, the tissue axial stretching model is analyzed theoretically. The theoretical result in a closed form indicates that the peak value of the cross-correlation function between the pre- and post-compression echoes is determined mainly by the beam width, the beam position and the lateral strain. Computer simulations are carried out to verify the theoretical conclusion. The theoretical analysis and simulation results can help to understand more clearly the decorrelation effect of tissue lateral displacements and the 2-D spatial comprehensive cross-correlation method presented previously to reduce the decorrelation effect.

Keywords: elastography, decorrelation, lateral displacements, the cross-correlation function, ultrasound.

Elastography, an ultrasonic technique for quantitatively imaging the elastic modulus distribution in soft tissues, is a promising method for the early detection of many tissue pathologies[1~3]. The internal tissue axial displacements resulting from a small, quasistatic external compression may be estimated using a cross-correlation analysis applied to the pre- and post-compression echo windows. The axial strain profile can be calculated from the gradient of the estimated displacements.

The performance of the displacement and strain estimation has been extensively analyzed[4~9]. Varghese et al. proposed a concept of strain filter as a theoretical framework to characterize the performance of elastography[6~9]. The strain filter concept indicates that the elastographic performance is limited by decorrelation noise induced by axial strain for large tissue strain values, and electronic noise for low strain values.

When tissue is compressed, ultrasonic scatterers in the tissue undergo a complex motion pattern that depends on the elastic properties and boundary conditions of the tissue. In addition to axial motions, lateral and elevational motions also introduce decorrelation to axial displacement estimation in elastography[8~10]. Since the sound beam is much broader in the elevational direction, the decorrelation effect of tissue elevational motions is usually not taken into account. As a result, the complex 3-D problem is simplified to a 2-D problem, usually a plane strain or a plane stress problem.

To study degradation of the elastographic quality introduced by the lateral and elevational motions of the scatterers, the concept of the strain filter was extended by Kallel et al.[8]. The effective cross-correlation function that includes the contributions of lateral and elevational decorrelation was used to estimate the decorrelation effect by both axial strain and non-axial displacements. Although the method of temporal stretching can significantly reduce the decorrelation effect induced by axial strain[11,12], stretching the post-compression echo also results in the stretching of the transducer point spread function (PSF), which also introduces decorrelation.

In our previous work, to estimate the decorrelation effect induced by tissue lateral displacements only, a tissue axial stretching model was presented to separate the coupling effects of axial strain and lateral displacements on decorrelation[13]. In this model, the post-compression tissue that undergoes a 2-D motion is stretched back to its original size in the axial direction, but remains in its post-compression position in the lateral direction. As a result, this axial stretching removes the axial strain and retains the lateral dis-

* Supported by the National Natural Science Foundation of China (Grant No. 60171039)

** To whom correspondence should be addressed. E-mail: deabj@tsinghua.edu.cn

placement. For a homogenous isotropic elastic tissue compressed by an infinite-width compressor with a perfect slip boundary, a scatterer in the position (x, y) will theoretically move to the position $((1+\varepsilon_x)x, (1-\varepsilon_y)y)$ after compression, where x and y are the lateral and axial direction of the transducer, the origin of the coordinate system is in the transducer center, ε_x and ε_y are the lateral and axial strain (absolute values), respectively, and $1+\varepsilon_x$ and $1-\varepsilon_y$ represent an expansion in the lateral direction and a compression in the axial direction, respectively. After tissue axial stretching, the scatterer will move to the position $((1+\varepsilon_x)x, y)$, which means that the coupling effect of axial strain is eliminated completely.

After separating the decorrelation effect induced by lateral displacements, the pre- and post-compression echoes are decomposed into two different parts, i.e. the signal part and the noise part. The signal part attributes to tissue scatterers remaining within the sound beam, while the noise part attributes to the move-in and move-out of tissue scatterers[13]. Therefore, the signal-to-noise ratio (SNR) can be used to analyze the decorrelation effect induced by lateral displacements.

As illustrated in our previous work, the decorrelation effect induced by lateral displacements decreases as the beam width increases, because the amount of scatterers remaining within the beam after compression increases as the beam width increases. The decorrelation effect induced by lateral displacements increases as the lateral strain increases or the ultrasound beam moves from the center of the transducer toward its edge[13]. It can be explained by that the total number of the scatterers remaining within the sound beam decreases with the increase of the lateral strain and the beam location.

The overall object of this study lies in the theoretical analysis of this already-presented tissue axial stretching model. After deriving a closed-form solution of the cross-correlation function between the pre- and post-compression echoes, the decorrelation effect that is dependent on the beam width, the beam position and the lateral strain, can be explained and predicted theoretically.

1 Model

A 2-D scanning model with a 1-D array transducer is used in this study. The echo obtained by the ultrasound beam located at x can be obtained as follows[13]:

$$s(x,y) = k(x,y) * p(x,y) = \iint k(x',y')p(x-x',y-y')\mathrm{d}x'\mathrm{d}y', \quad (1)$$

where $k(x, y)$ represents the scattering response of the discrete scatterers, $p(x, y)$ is the PSF at the focal zone of the array transducer, '$*$' denotes the convolution operation, x and y are the lateral and axial coordinates, respectively.

The scattering response $k(x, y)$ can be described as follows[13]:

$$k(x,y) = K_s \cdot \sum_{i=1}^{n} d_i \cdot \delta(x-x_i, y-y_i), \quad (2)$$

where K_s is the scattering constant coefficient, d_i is the diameter of the ith scatterer, n is the total number of scatterers within the tissue, and $\delta(x, y)$ denotes the 2-D Dirac delta function, (x_i, y_i) represents the space location of the ith scatterer. In this work, the scatterer location in the tissue is taken as a 2-D (spatial) Poisson process, whose intensity represents the average density of scatterers[14,15], and the scatterer diameter is taken as a normal distribution. In this model, all of the scatterers are considered to be point reflectors and the multiple scattering is ignored. Here the scattering response is simplified to be proportional to the scatterer diameter ($k \propto d$). More generally, the scattering response is assumed to be proportional to the scatterer diameter powered to q ($k \propto d^q, 1 \leqslant q \leqslant 3$), where q is a medium dependent constant[16]. However, the exact value of q is not important in the analysis here. In addition, the frequency dependence of the scattering response is not considered for simplifying the problem.

In the focal area, the PSF may be modeled by the following separable form[13,17,18]:

$$p(x,y) = p_l(x)p_a(y), \quad (3)$$

where $p_a(y)$ and $p_l(x)$ are the axial and lateral PSF components, respectively. In this work, $p_a(y)$ is assumed to be a zero mean Gaussian modulated cosine pulse. The lateral PSF component of an unapodized, rectangular transducer aperture (not considering grating lobes) is given by[13,17,18]

$$p_l(x) = \begin{cases} \left(\dfrac{\sin\left[\frac{\pi x}{w/2}\right]}{\left[\frac{\pi x}{w/2}\right]}\right)^2 & -\dfrac{w}{2} \leqslant x < \dfrac{w}{2}, \\ 0 & \text{otherwise}, \end{cases} \quad (4)$$

where w denotes the transducer beam width.

2 Theory

In elastography, there are two major noise sources affecting the performance of axial time delay (i.e. axial displacement) estimation: the random electronic noise of ultrasonic instruments and the decorrelation noise. Both of them can reduce the peak value of the cross-correlation function between the pre- and post-compression echoes. The electronic noise can be characterized by the sonographic SNR. If a signal $s_1(y)$ and its delay version $s_2(y)$ are corrupted by uncorrelated noise, the peak value of the cross-correlation function is related to a correlation SNR by[19]

$$\mathrm{SNR}_\rho = \frac{R_{s_1,s_2}(y_0)}{1 - R_{s_1,s_2}(y_0)}, \tag{5}$$

where $R_{s_1,s_2}(y_0)$ denotes the peak value of the energy-normalized cross-correlation function between $s_1(y)$ and $s_2(y)$, and y_0 is the time delay of $s_2(y)$ relative to $s_1(y)$. It can be seen from Eq. (5) that the value of correlation SNR increases nonlinearly as the peak value of the cross-correlation function increases.

In our previous work, the pre- and post-compression echoes can be decomposed into two uncorrelated parts, i.e. the signal part and the noise part. In the tissue axial stretching model, the time delay is equal to zero. Because the decorrelation noise introduced by tissue lateral displacements reduces the peak value of the cross-correlation function, as well as the electronic noise, the decorrelation noise may be equivalent to an electronic noise using the same relation as Eq. (5). Thus the decorrelation can be characterized by the peak value of the cross-correlation function between the pre- and post-compression echoes ($R_{s_1,s_2}(0)$).

In Appendix A, the cross-correlation function is theoretically deduced in detail, on the assumption that a homogenous isotropic tissue is compressed by an infinite compressor with a perfect slip boundary, and stretched back in the axial direction. To obtain the analytical expression of the cross-correlation function, the area of integral calculation in Eq. (1) is divided into lots of nonoverlapping thin strips. The echo from a strip can be regarded as the output of a compound Poisson impulse process passing a linear filter. According to the properties of a linear filter, the cross-correlation function between the pre- and post-compression echoes from the strip becomes the cross-correlation function between the pre- and post-compression compound Poisson impulse process convolving the auto-correlation of the filter impulse response. Summing the cross-correlation function between the pre- and post-compression echoes from all strips, the cross-correlation function is obtained as follows:

$$R_{s_1,s_2}(y) = \frac{\int p_l(l_j - x_1)p_l(l_j - (1+\varepsilon_x)x_1)\mathrm{d}x_1}{\sqrt{\int p_l^2(l_j - x_1)\mathrm{d}x_1 \cdot \int p_l^2(l_j - (1+\varepsilon_x)x_1)\mathrm{d}x_1}} \cdot \frac{R_{p_a}(y)}{R_{p_a}(0)}, \tag{6}$$

where $R_{s_1,s_2}(y)$ represents the energy-normalized cross-correlation function between the pre-compression echo ($s_1(y)$) and the post-compression echo ($s_2(y)$) in tissue axial stretching model, l_j and ε_x represent the beam position and the lateral strain, $R_{p_a}(y)$ is the auto-correlation function of the axial PSF component ($p_a(y)$):

$$R_{p_a}(y) = \int p_a(y')p_a(y'+y)\mathrm{d}y'. \tag{7}$$

Thus the peak value of the cross-correlation function is obtained as

$$R_{s_1,s_2}(0) = \frac{\int p_l(l_j - x_1)p_l(lj - (1+\varepsilon_x)x_1)\mathrm{d}x_1}{\sqrt{\int p_l^2(l_j - x_1)\mathrm{d}x_1 \cdot \int p_l^2(lj - (1+\varepsilon_x)x_1)\mathrm{d}x_1}}. \tag{8}$$

In Eqs. (6) and (8), the term $p_l(l_j - x_1)$ can be attributed to a scatterer in lateral position x_1 to the pre-compression echo; and the term $p_l(l_j - (1+\varepsilon_x)x_1)$ can be attributed to this scatterer to the post-compression echo. Therefore, $p_l(l_j - x_1)p_l(l_j - (1+\varepsilon_x)x_1)\mathrm{d}x_1$ can be considered to be the contribution of this scatterer to the amplitude of the cross-correlation function; and the integral $\int p_l(l_j - x_1)p_l(l_j - (1+\varepsilon_x)x_1)\mathrm{d}x_1$ denotes the overall contribution of all tissue scatterers. The term $\sqrt{\int p_l^2(l_j - x_1)\mathrm{d}x_1 \cdot \int p_l^2(l_j - (1+\varepsilon_x)x_1)\mathrm{d}x_1}$ denotes the normalization by the energy of the pre- and post-compression echoes.

In Eqs. (6) and (8), the x_1 coordinate is relative to the transducer symmetric axis. To simplify

Eq. (8), let $x = x_1 - l_j$. It means that the coordinate axis of x_1 moves to the center of the beam (beam position). Using the even symmetry of $p_l(x)$ given by Eq. (4), Eq. (8) is rewritten as

$$R_{s_1,s_2}(0) = \frac{\int p_l(x)p_l(x + \varepsilon_x l_j + \varepsilon_x x)\mathrm{d}x}{\sqrt{\int p_l^2(x)\mathrm{d}x \cdot \int p_l^2(x + \varepsilon_x l_j + \varepsilon_x x)\mathrm{d}x}}. \quad (9)$$

There is an implicit term that influences the peak value of the cross-correlation function given by Eq. (9). It can be seen from Eq. (4) that the beam width determines the lateral PSF component of the transducer ($p_l(x)$). Thus the beam width (w) is one of the factors that influence the cross-correlation function, as well as the beam position (l_j) and the lateral strain (ε_x).

3 Simulation

Simulation experiment has been carried out to test the theory presented in this work. The scatterer spatial distribution in the tissue is taken as a 2-D Poisson process, where the intensity λ represents the average density of tissue scatterers[14,15]. In this paper, the average density of scatterers (λ) is equal to 16/mm^2, the length and width of the tissue are both set to be 60 mm. The scatterer diameter is simulated as a truncated normal distribution with an average of 0.05 mm, a standard deviation of 0.01 mm, a minimum of 0.01 mm and a maximum of 0.10 mm.

The array transducer is modeled by a center frequency f_0 of 3.5 MHz, and a bandwidth defined by the quality factor $Q = 3.5$. The quality factor Q is defined as $Q = f_0/\Delta f$, where Δf is the bandwidth at half-power (-3 dB bandwidth) in the power spectrum of the lateral PSF component ($p_a(y)$).

The tissue is simulated as a homogenous isotropic elastic medium. When an axial strain ε_y is applied, the tissue undergoes a lateral strain $\varepsilon_x = \upsilon\varepsilon_y$, where υ is the Poisson's ratio. The simulation of 2-D compression and axial stretching can be simplified to compress merely in the lateral direction with the lateral strain ε_x. The speed of sound in the medium is set at a constant value of 1540 m/s and the sampling rate of ultrasonic echoes is 40 MHz. According to the pre- and post-compression positions of tissue scatterers, the pre- and post-compression echoes are calculated from Eq. (1). Here the ultrasonic random noise is not taken into account. The echo windows are separated to be nonoverlapping and 3 mm in window length. The simulation results are achieved from the average of 50 independent simulations.

Fig. 1 presents the cross-correlation function in theory and simulation. The beam width, the beam position and the lateral strain are 1.5 mm, 15 mm and 0.004, respectively. It seems that the results in simulation are close to that in theory.

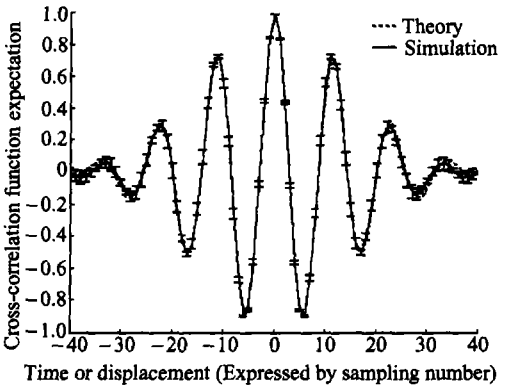

Fig. 1. The cross-correlation function in theory and simulation. Parameters: lateral strain $\varepsilon_x = 0.004$; beam position $l_j = 15$ mm; beam width $w = 1.5$ mm.

Fig. 2 shows the peak value of the cross-correlation function both in simulation and direct calculation of Eq. (9) using the numerical integral method, with different beam positions and lateral strains. As the beam position increases, the peak value of the cross-correlation function decreases steadily, particularly with a larger lateral strain.

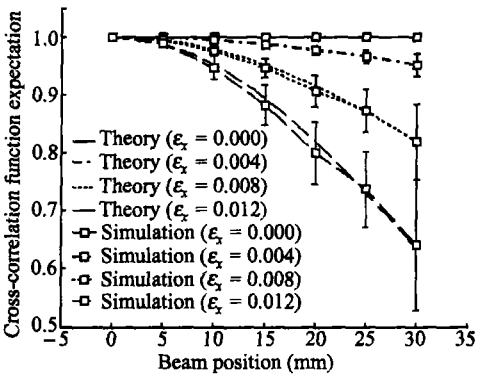

Fig. 2. The peak value of the cross-correlation function both in theory and simulation with different beam positions and lateral strains. Parameters: lateral strain ε_x is from 0.000 to 0.012 by an increment of 0.004; beam position l_j is from 0 to 30 mm by an increment of 5 mm and beam width w is 1.5 mm.

Fig. 3 represents the peak value of the cross-correlation function in simulation and theory with different lateral positions and beam widths. The peak value of the cross-correlation function with a narrower beam drops much more rapidly with the increasing of the beam position than that with a broader beam.

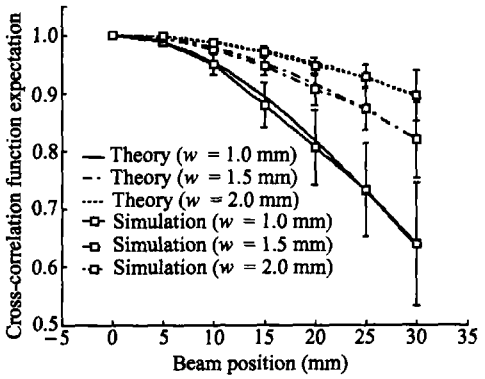

Fig. 3. The peak value of the cross-correlation function both in theory and simulation with different beam widths and beam positions. Parameters: beam width w is 1.0, 1.5 and 2.0 mm; beam position l_j is from 0 to 30 mm by an increment of 5 mm and lateral strain ε_x is 0.008.

4 Discussions and conclusion

Since the correlation SNR in the pre- and post-compression echoes is directly related to the peak value of the cross-correlation function[19], the latter term can be used to characterize the decorrelation effect induced by lateral displacements in the tissue axial stretching model. The theoretical closed-form solution and the simulation results indicate that the beam width, the beam position and the lateral strain are main impact parameters of decorrelation effect induced by tissue lateral displacements, as can be seen from Fig. 2 and Fig. 3.

When ultrasound beam is far enough from transducer symmetric axis, i.e. $l_j \gg w$, Eq. (9) can be rewritten as

$$R_{s_1,s_2}(0) = \frac{\int p_l(x)\,p_l(x+\varepsilon_x l_j)\,\mathrm{d}x}{\sqrt{\int p_l^2(x)\,\mathrm{d}x \cdot \int p_l^2(x+\varepsilon_x l_j)\,\mathrm{d}x}}. \tag{10}$$

Because it satisfies $\int p_l^2(x+\varepsilon_x l_j)\,\mathrm{d}x = \int p_l^2(x)\,\mathrm{d}x$, Eq. (10) can be rewritten as

$$R_{s_1,s_2}(0) = \frac{\int p_l(x)\,p_l(x+\varepsilon_x l_j)\,\mathrm{d}x}{\int p_l^2(x)\,\mathrm{d}x}, \tag{11}$$

where the beam position and the lateral strain are united to one parameter, i.e. the lateral displacement. As the lateral displacement increases, the peak value of the cross-correlation function decreases. That is to say, the decorrelation of pre- and post-compression echoes induced by lateral displacements increases. Because the beam is relatively narrow in practice, it satisfies $l_j \gg w$ in most positions except those near the transducer center. Thus Eq. (11) can be a more simple solution to express the decorrelation effect. This result is similar to that given by Kallel et al.[10], where the tissue scattering function was simply modeled as a white Gaussian random process, and the lateral displacements within the sound beam were assumed to be constant.

When the lateral displacement is greater than the beam width, namely,

$$(1+\varepsilon_x)\left(l_j - \frac{w}{2}\right) \geqslant l_j + \frac{w}{2}, \tag{12}$$

or

$$l_j \geqslant \frac{w(2+\varepsilon_x)}{2\varepsilon_x}, \tag{13}$$

where $l_j - \frac{w}{2}$ and $l_j + \frac{w}{2}$ are two boundaries of the jth beam, the peak value of the cross-correlation function turns to be zero:

$$R_{s_1,s_2}(0) = 0, \tag{14}$$

which means that the pre- and post-compression echoes become decorrelated completely. Since the lateral strain is small enough in elastography, it satisfies $\frac{w(2+\varepsilon_x)}{2\varepsilon_x} \approx \frac{w}{\varepsilon_x}$. Then Eq. (13) becomes $\varepsilon_x l_j \geqslant w$, where $\varepsilon_x l_j$ is approximately equal to the lateral displacement of tissues within the jth sound beam. Sometimes, complete decorrelation may be encountered in elastography, especially when the lateral strain is relatively large. For example, if the beam width $w = 1.5$ mm and the lateral strain $\varepsilon_x = 0.05$, the pre- and post-compression echoes obtained at the beam $l_j \geqslant 30$ mm are completely decorrelated. In these situations, all the scatterers in the sound beam before compression move out after compression. Thus tissue axial displacements cannot be estimated through the cross-correlation function between the pre- and post-compression echoes, unless the correction of tissue lateral displacements has been consid-

ered[18,20].

The newly-developed tissue axial stretching model separates the decorrelation effect induced by lateral displacements from other decorrelation sources. The theoretical analysis in this paper helps to understand more distinctly the decorrelation effect and the dependence of some parameters, including the beam width, the beam position and the lateral strain. It is shown that the decorrelation noise induced by tissue lateral displacements may be reduced by decreasing the lateral strain, using the central beams of the transducer and applying relatively narrow ultrasound beams. However, these methods are quite limited and not practical in most practical situations. For example, decreasing the lateral strain also decreases the SNR in elastography since the axial strain also decreases in practice. Using only the central beams reduces the detective range available in elastography.

Therefore, a 2-D spatial comprehensive cross-correlation method was proposed in our previous work to reduce the decorrelation noise induced by tissue lateral displacements[13]. This method sums the cross-correlation functions from several adjacent beams to obtain a comprehensive cross-correlation function. The decorrelation noise induced by tissue lateral displacements decreases as the total number of adjacent beams used increases.

The performance of the 2-D spatial comprehensive cross-correlation method can be explained well by the theoretical analysis in this study. The 2-D spatial comprehensive cross-correlation method uses the sum of several cross-correlation functions from adjacent beams to estimate the axial displacements. The more adjacent beams are used to calculate the cross-correlation function, the more information about the ultrasonic scatterers is included within the echoes. It can be regarded as using a single beam but with a wider beam when using more adjacent beams in calculating the cross-correlation function.

The tissue axial stretching model is a theoretical model used to understand the decorrelation effect of lateral displacements. However, in practice, to verify the theoretical results in this paper it is quite difficult to achieve the axial stretching of tissue (or phantom). An approximate approach is to move the homogeneous tissue or transducer along the lateral direction of the transducer, but not to compress the target. This is because the theoretical analysis demonstrates that the decorrelation effect in a certain transducer (with a constant beam width) is mainly decided by the lateral displacements, as indicated previously in the discussions. However, the theoretical analysis here can help to understand more clearly the decorrelation effect induced by lateral displacements, the tissue axial stretching model, and the effect of 2-D comprehensive cross-correlation function as well.

Appendix A Theoretical deduction of cross-correlation function

1 Definition of the cross-correlation function

The cross-correlation function between pre- and post-compression echoes in tissue axial stretching model is defined as

$$R_{s_1,s_2}(y) = \left\langle \frac{1}{T}\int_T s_1(y')s_2(y'+y)\mathrm{d}y' \right\rangle, \tag{A1}$$

where $s_1(y)$ and $s_2(y)$ are the pre-compression echo and post-compression echo (after tissue axial stretching, the same below), respectively, T is the window length, and $\langle\cdot\rangle$ denotes the ensemble average operation.

2 Discretization of scattering echoes

The scattering echo of the jth beam is given by

$$s(l_j,y) = \iint k(x',y')p_l(l_j-x')p_a(y-y')\mathrm{d}x'\mathrm{d}y', \tag{A2}$$

where l_j denotes the lateral position of the beam.

To obtain the analytical expression of the cross-correlation function, the area for integration in (A2) is divided into many nonoverlapping thin strips, as show in Fig. A1 (a) and (b), before and after compression, respectively. The pre-compression echo from the strip located at x_1 with width $\mathrm{d}x_1$ can be expressed as

$$\begin{aligned}\mathrm{d}s_1(l_j,y)\mid_{x_1} &= \int\left[\int_{x_1}^{x_1+\mathrm{d}x_1} k(x',y')p_l(l_j-x')\mathrm{d}x'\right] \\ &\quad \cdot p_a(y-y')\mathrm{d}y' \\ &= \mathrm{d}k_1(l_j,y)\mid_{x_1} * p_a(y),\end{aligned} \tag{A3}$$

where

$$\mathrm{d}k_1(l_j,y)\mid_{x_1} = \int_{x_1}^{x_1+\mathrm{d}x_1} k(x',y)p_l(l_j-x')\mathrm{d}x'. \tag{A4}$$

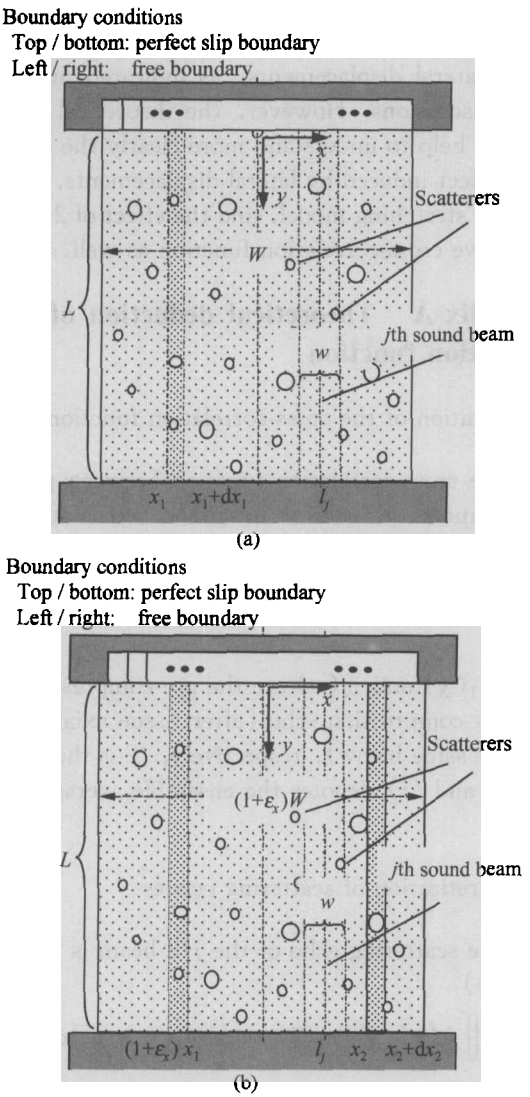

Fig. A1. The diagrammatic sketch of tissue discretization before compression (a), and after compression and axial stretching (b).

Assuming dx_1 is small enough, $dk_1(y)|_{x_1}$ can be represented approximately as

$$dk_1(l_j, y)|_{x_1} \approx p_l(l_j - x_1)\int_{x_1}^{x_1+dx_1} k(x', y)dx'. \quad (A5)$$

Substituting (2) into the latter term in (A5) and using the separability of 2-D Dirac delta function, we obtain

$$\int_{x_1}^{x_1+dx_1} k(x', y)dx' = \int_{x_1}^{x_1+dx_1}\left[\sum_i K_s d_{i,1}\delta(x' - x_{i,1}, y - y_{i,1})\right]dx' = \sum_i\left[\int_{x_1}^{x_1+dx_1} K_s d_{i,1}\delta(x' - x_{i,1}, y - y_{i,1})dx'\right] = \sum_{x_{i,1}\in[x_1, x_1+dx_1)} K_s d_{i,1}\delta(y - y_{i,1}), \quad (A6)$$

where K_s is a scattering constant coefficient, $d_{i,1}$ is the diameter of the ith scatterer which is located at $(x_{i,1}, y_{i,1})$ before compression.

Thus the integral in (A5) is expressed as the sum of scattering function of individual scatterers within the strip $[x_1, x_1 + dx_1)$. In this paper, the scatterer position distribution in the tissue is simulated as a 2-D Poisson process. Therefore, the distribution of the scatterers within $[x_1, x_1 + dx_1)$ along y direction can be regarded as a 1-D Poisson process with an intensity of λdx_1. Since the scatterer diameters which determine the scattering strength have the same normal distribution, the scattering function (A6) can be regarded as a compound Poisson process with an intensity of λdx_1 and a marked value of $K_s d_i$. Then (A5) can be regarded as a compound Poisson process with an intensity of $\lambda_1 = \lambda dx_1$ and a marked value of $p_x(l_j - x)\cdot K_s d_i$. Thus (A3) can be regarded as the output of the compound Poisson impulse process (A5) passing a linear filter with an impulse response of $p_a(y)$.

After compression and tissue axial stretching, the strip width becomes

$$dx_2 = (1 + \varepsilon_x)dx_1. \quad (A7)$$

Because the tissue volume (distribution space of scatterers) increases with ε_x after compression and tissue axial stretching, the intensity of 2-D Poisson process of scatterers becomes $\frac{\lambda}{1+\varepsilon_x}$.

In a similar way, the post-compression scattering echo from the strip located at x_2 can be represented as

$$ds_2(l_j, y)|_{x_2} = dk_2(l_j, y)|_{x_2} * p_a(y), \quad (A8)$$

where

$$dk_2(l_j, y)|_{x_2} \approx p_l(l_j - x_2)\int_{x_2}^{x_2+dx_2} k(x', y)dx', \quad (A9)$$

$$\int_{x_2}^{x_2+dx_{21}} k(x', y)dx' = \sum_{x_{i,2}\in[x_2, x_2+dx_2)} K_s d_{i,2}\delta(y - y_{i,2}). \quad (A10)$$

Similar to (A5), (A9) can be regarded as a compound Poisson process with an intensity of $\lambda_2 = \frac{\lambda}{1+\varepsilon_x}dx_2 = \lambda dx_1 = \lambda_1$ and a marked value of $p_x(l_j - x)\cdot K_s d_i$. Thus (A8) can be regarded as the output

of the compound Poisson (A9) passing a linear filter with an impulse response of $p_a(y)$.

The pre- and post- compression echoes received by the jth beam can be expressed as the sum of scattering echo signals from all strips:

$$s_1(l_j, y) = \sum \mathrm{d}s_1(l_j, y)\mid_{x_1} \to \int_{x_1} \mathrm{d}s_1(l_j, y)\mid_{x_1} \quad \text{as } \mathrm{d}x_1 \to 0, \tag{A11}$$

$$s_2(l_j, y) = \sum \mathrm{d}s_2(l_j, y)\mid_{x_2} \to \int_{x_2} \mathrm{d}s_2(l_j, y)\mid_{x_2} \quad \text{as } \mathrm{d}x_2 \to 0. \tag{A12}$$

Then the cross-correlation function (A1) becomes

$$\begin{aligned} R_{s_1, s_2}(y) &= \left\langle \frac{1}{T}\int_T \left(\int_{x_1} \mathrm{d}s_1(l_j, y')\mid_{x_1}\mathrm{d}x_1 \cdot \int_{x_2} \mathrm{d}s_2(l_j, y' + y)\mid_{x_2}\mathrm{d}x_2 \right) \mathrm{d}y' \right\rangle \\ &= \int_{x_1}\int_{x_2} \left\langle \frac{1}{T}\int_T \mathrm{d}s_1(l_j, y')\mid_{x_1} \cdot \int_{x_2} \mathrm{d}s_2(l_j, y' + y)\mid_{x_2}\mathrm{d}y' \right\rangle \mathrm{d}x_1\mathrm{d}x_2 \\ &= \int_{x_1}\int_{x_2} R_{\mathrm{d}s_1, \mathrm{d}s_2}(y)\mathrm{d}x_1\mathrm{d}x_2. \end{aligned} \tag{A13}$$

Thus the calculation of the cross-correlation function $R_{s_1, s_2}(y)$ turns to the calculation of the discretized cross-correlation function $R_{\mathrm{d}s_1, \mathrm{d}s_2}(y)$.

3 Deduction of cross-correlation function

There are two cases to be considered for the computation of $R_{\mathrm{d}s_1, \mathrm{d}s_2}(y)$ in (A13). In one case, the pre- and post-compression strips contain the same scatterers. In the other case, the pre- and post-compression strips contain different scatterers. These two cases are discussed as below:

(1) When $x_2 = (1 + \varepsilon_x)x_1$, the scatterers in the strip located at x_2 after compression are the same as that in the strip located at x_1 before compression:

$$\sum_{x_{i,1} \in [x_1, x_1 + \mathrm{d}x_1)} K_s \mathrm{d}_{i,1}\delta(y - y_{i,1}) = \sum_{x_{i,2} \in [x_2, x_2 + \mathrm{d}x_2)} K_s d_{i,2}\delta(y - y_{i,2}). \tag{A14}$$

The cross-correlation function between (A4) and (A9) can be regarded as the cross-correlation function between the same compound Poisson process with different marked label, which can be expressed as follows[15]:

$$R_{\mathrm{d}k_1, \mathrm{d}k_2}(y) = p_l(l_j - x_1)p_l(l_j - x_2) \cdot K_s^2[D_d\lambda_1\delta(y) + m_d^2\lambda_1^2], \tag{A15}$$

where D_d and m_d are the mean-square and the expectation of d_i, respectively.

As a result, according to the property of the linear shift invariant system[15], the cross-correlation function between echoes of (A3) and (A8) is given by

$$\begin{aligned} R_{\mathrm{d}s_1, \mathrm{d}s_2}(y) &= R_{\mathrm{d}k_1, \mathrm{d}k_2}(y) * p_a(y) * p_a(-y) \\ &= p_l(l_j - x_1)p_l(l_j - x_2) \cdot K_s^2 \left\{ D_d\lambda\,\mathrm{d}x_1\int_{-\infty}^{\infty} p_a(y')p_a(y' + y)\mathrm{d}y' + m_d^2\lambda_1^2\left[\int p_a(y)\mathrm{d}y\right]^2 \right\}. \end{aligned} \tag{A16}$$

(2) When $x_2 \neq (1 + \varepsilon_x)x_1$, the scatterers in the strip located at x_2 after compression is different from that in the strip located at x_1 before compression. Thus, the cross-correlation function between two scattering functions (A4) and (A9) can be regarded as the cross-correlation function between different compound Poisson processes, which can be expressed as follows[15]:

$$R_{\mathrm{d}k_1, \mathrm{d}k_2}(y) = p_l(l_j - x_1)p_l(l_j - x_2) \cdot K_s^2 m_d^2\lambda_1^2. \tag{A17}$$

Then the cross-correlation function between echoes (A3) and (A8) is given by

$$\begin{aligned} R_{\mathrm{d}s_1, \mathrm{d}s_2}(y) &= R_{\mathrm{d}k_1, \mathrm{d}k_2}(y) * P_a(y) * P_a(-y) \\ &= p_l(l_j - x_1)p_l(l_j - x_2) \cdot K_s^2 m_d^2\lambda_1^2\left[\int p_a(y')\mathrm{d}y'\right]^2. \end{aligned} \tag{A18}$$

Considering $p_a(y)$ is a zero mean function and combining (A16) and (A18), the cross-correlation function between echoes of (A3) and (A8) is given by

$$R_{\mathrm{d}s_1\mathrm{d}s_2}(y) = \begin{cases} p_l(l_j - x_1)p_l(l_j - x_2) \cdot K_s^2 D_d\lambda\,\mathrm{d}x_1\int_{-\infty}^{\infty} p_a(y')p_a(y' + y)\mathrm{d}y' & x_2 = (1 + \varepsilon_x)x_1, \\ 0 & x_2 \neq (1 + \varepsilon_x)x_1. \end{cases} \tag{A19}$$

Using (A19), the cross-correlation function (A13) can be expressed as

$$R_{s_1,s_2}(y) = \left[\int p_l(l_j - x_1)p_l(l_j - (1+\varepsilon_x)x_1)\mathrm{d}x_1\right] \cdot K_s^2 D_d \lambda \cdot R_{p_a}(y), \quad \text{(A20)}$$

where $R_{p_a}(y)$ denotes the auto-correlation function of $p_a(y)$:

$$R_{p_a}(y) = \int p_a(y')p_a(y'+y)\mathrm{d}y'. \quad \text{(A21)}$$

Here the average and normalization are omitted in the calculation of the auto-correlation function since $R_{p_a}(y)$ is a deterministic energy signal.

Note that the cross-correlation function is normalized by the window length, as shown in (A1). In axial displacement estimation, the cross-correlation function is typically normalized by energy:

$$R_{s_1,s_2}(y) = \left\langle \frac{\int_T s_1(y')s_2(y'+y)\mathrm{d}y'}{\sqrt{\int_T s_1^2(y')\mathrm{d}y' \cdot \int_2 s_2^2(y')\mathrm{d}y'}} \right\rangle. \quad \text{(A22)}$$

Then the cross-correlation function (A20) can be expressed as an energy-normalized form:

$$R_{s_1,s_2}(y) = \frac{\int p_l(l_j - x_1)p_l(l_j - (1+\varepsilon_x)x_1)\mathrm{d}x_1}{\sqrt{\int p_l^2(l_j - x_1)\mathrm{d}x_1 \cdot \int p_l^2(l_j - (1+\varepsilon_x)x_1)\mathrm{d}x_1}} \cdot \frac{R_{p_a}(y)}{R_{p_a}(0)}. \quad \text{(A23)}$$

In the procedure of theoretical derivation, we do not suppose the shape of the axial PSF ($P_a(y)$) beforehand, except its zero mean character. This zero-mean assumption is reasonable for two reasons. Firstly, the axial PSF is approximately zero in most cases. Secondly, in elastography, a general preprocessing is to center the pre- and post-compression echoes, i.e. subtract their means respectively so as to make them zero-mean echoes. In addition, the shape of the lateral PSF ($P_l(x)$) can be arbitrary here. In the main text, the lateral PSF has been assumed to be a truncated function only for simplification in simulation and analysis.

References

1 Ophir, J. et al. Elastography: a quantitative method for imaging the elasticity of biological tissues. Ultrasonic Imaging, 1991, 13 (2): 111.

2 Ophir, J. et al. Elastography: ultrasonic estimation and imaging of the elastic properties of tissues. In: Proceedings of the Institution of Mechanical Engineers, Part H- Journal of Engineering in Medicine, 1999, 213(H3): 203.

3 Ophir, J. et al. Elastography. Comptes Rendus De L Academie Des Sciences Serie IV Physique Astrophysique, 2001, 2(8): 1193.

4 Bilgen, M. et al. Error analysis in acoustic elastography. 1. Displacement estimation. Journal of the Acoustical Society of America, 1997, 101(2): 1139.

5 Bilgen, M. et al. Error analysis in acoustic elastography. 2. Strain estimation and SNR analysis. Journal of the Acoustical Society of America, 1997, 101(2): 1147.

6 Varghese, T. et al. A theoretical framework for performance characterization of elastography: The strain filter. IEEE Transactions on Ultrasonics Ferroelectrics and Frequency Control, 1997, 44 (1): 164.

7 Kallel, F. et al. The nonstationary strain filter in elastography. 2. Lateral and elevational decorrelation. Ultrasound in Medicine and Biology, 1997, 23(9): 1357.

8 Varghese, T. et al. The nonstationary strain filter in elastography. 1. Frequency dependent attenuation. Ultrasound in Medicine and Biology, 1997, 23(9): 1343.

9 Varghese, T. et al. Tradeoffs in elastographic imaging. Ultrasonic Imaging, 2001, 23(4): 216.

10 Kallel, F. et al. Three-dimensional tissue motion and its effect on image noise in elastography. IEEE Transactions on Ultrasonics Ferroelectrics and Frequency Control, 1997, 44(6): 1286.

11 Céspedes, I. et al. Reduction of image noise in elastography. Ultrasonic Imaging, 1993, 15(2): 89.

12 Varghese, T. et al. Enhancement of echo-signal correlation in elastography using temporal stretching. IEEE Transactions on Ultrasonics Ferroelectrics and Frequency Control, 1997, 44(1): 173.

13 Bai, J. et al. Estimation and reduction of decorrelation effect induced by tissue lateral displacement in elastography. IEEE Transactions on Ultrasonics Ferroelectrics and Frequency Control, 2002, 49(5): 541.

14 Snyder, D. L. Random Point Processes, New York: Wiley, 1975.

15 Yang, F. S. Random Signal Analysis, Beijing: Tsinghua University Press (in Chinese), 1990.

16 Ingard, K.U. et al. Theoretical Acoustics, New York: McGraw-Hill, 1968.

17 Wagner, R. et al. Statistics of speckle in ultrasound B-scans. IEEE Transactions on Ultrasonics Ferroelectrics and Frequency Control, 1983, 30(3): 156.

18 Konofagou, E. et al. A new elastographic method for estimation and imaging of lateral displacements, lateral strains, corrected axial strains and Poisson's ratios in tissues. Ultrasound in Medicine and Biology, 1998, 24(8): 1183.

19 Céspedes, I. et al. The combined effect of signal decorrelation and random noise on the variance of time delay estimation. IEEE Transactions on Ultrasonics Ferroelectrics and Frequency Control, 1997, 44(1): 220.

20 Chaturvedi, P. et al. 2-D companding for noise reduction in strain imaging. IEEE Transactions on Ultrasonics Ferroelectrics and Frequency Control, 1998, 45(1): 179.